Original Article

The novel model: Experimental optical coherence tomography–guided anterior segment imaging chick embryo model

Resat Duman, Tolga Ertekin[1], Rahmi Duman, Esra Aslan[2], Mehmet Cem Sabaner, Ersan Çetinkaya[3]

Purpose: The aim of this study was to present an experimental optical coherence tomography (OCT)–guided anterior segment (AS) imaging chick embryo model. Through this model, we aimed to reveal similarities and differences between human cornea, AS tissues, and chick embryo tissues by quantitative image analysis. **Methods:** *Ex vivo*, the chick embryos' globes were determined by detailed AS camera of spectral-domain (SD)-OCT in 10 fertilized specific pathogen-free eggs on the 20th day. Quantitative image analysis of anterior chamber tissues was performed with SD-OCT in detail. After imaging, cross sections of the chick embryo globes containing cornea with anterior chamber were histologically examined and compared with human tissues. The similarities of our model with data in the human cornea and AS studies in the literature were compared. **Results:** SD-OCT imaging was able to successfully delineate the AS tissues of chick embryos such as the cornea, iris, lens, pupil, conjunctiva, ciliary body, anterior chamber, and lens. Quantitative semi-automated measurements showed the following: mean central corneal thickness: 213.4 ± 7.05 μm (197–223 μm), mean anterior chamber depth: 878.9 ± 41.74 (804–919 μm), mean anterior chamber area: 2.43 ± 0.16 mm^2 ($2.17–2.73 mm^2$), mean corneoscleral junction (limbal) thickness: 322.8 ± 20.05 μm (289–360 μm), and mean iris thickness: 230.4 ± 13.27 μm (203–245 μm). In addition, detailed histological comparisons of the AS tissues with human tissues were evaluated to be very similar. **Conclusion:** In conclusion, this chick embryo model mimics human tissues and it can be considered as a platform for the study of teratogen-induced malformations and AS dysgenesis during gestation of AS tissues. In addition, this study demonstrates the feasibility of SD-OCT in the quantitative assessment of AS structures in chick embryo model.

Access this article online

Website: www.ijo.in

DOI: 10.4103/ijo.IJO_263_18

Quick Response Code:

Keywords: Anterior segment, chick embryo, cornea, experimental animal model, spectral-domain optical coherence tomography

Animal models of the anterior segment (AS) of the eye are important for both understanding the pathologies and testing potential preventative therapeutics. Numerous animal models (mouse, rabbit, rat, guinea pig, zebra fish, chick embryo, dog, cat, bovine, monkey) have been developed for investigation of normal eye development and various corneal and AS pathologies.[1-6]

Various imaging modalities [optical coherence tomography (OCT), confocal microscopy, and ultrasound biomicroscopy] are applied to understand the pathologies of corneal diseases in animals. Spectral-domain (SD)-OCT is used as a cross-sectional, noncontact high-resolution imaging technique that can be safely used for diagnosis and follow-up with tomographic imaging of cornea, iris, lens, pupil, conjunctiva, ciliary body, anterior chamber, aqueous humor, and lens.

To the best of our knowledge, this is the first study reporting experimental OCT-guided AS imaging model in chick embryos. In this study, we examined whether chick embryo AS tissues and human AS tissues are similar in terms of anatomical, morphological, and histopathological characteristics with OCT images and investigated the suitability of chick embryo AS model as an experimental model. Through this model, we aimed to reveal similarities and differences between human AS tissues and chick embryo tissues.

Methods

Animals

A total of 10 fertilized specific pathogen-free (SPF) eggs were used for this study. All SPF eggs were placed in the incubator and monitored in the incubator at 37.5°C and 68% relative humidity. The first day of incubation was designated as day 1. On the 20th day, SPF eggs were removed from the incubator. All embryos were sacrificed and chick eyes were removed from chick embryos under the dissection microscope. Only animals with normal AS and cornea were included in the study. This

Department of Ophthalmology, [1]Anatomy and [2]Histology-Embryology, School of Medicine, Afyon Kocatepe University, Afyonkarahisar, [3]Department of Ophthalmology, Antalya Education and Research Hospital, Antalya, Turkey

Correspondence to: Dr. Resat Duman, Department of Ophthalmology, School of Medicine, Afyon Kocatepe University, Afyonkarahisar, Turkey. E-mail: resatduman@gmail.com

Manuscript received: 22.02.18; Revision accepted: 08.08.18

Cite this article as: Duman R, Ertekin T, Duman R, Aslan E, Sabaner MC, Çetinkaya E. The novel model: Experimental optical coherence tomography–guided anterior segment imaging chick embryo model. Indian J Ophthalmol 2019;67:54-8.

study protocol has been approved by institutional animal research ethics committe and all experiments were conducted in accordance with the animal research protocol of Afyon Kocatepe University Ethics Committee (approval number: AKUHADYEK-235-17).

SD-OCT measurements

Each globe was placed and secured in a pad within the normal anatomical position. Corneal protection was provided with a topical balanced salt solution. *Ex vivo* AS imaging was performed with SD-OCT (Spectralis Heidelberg Engineering GmbH, Heidelberg, Germany) for all right eyes of the chick embryos. Comparisons among SD-OCT images of human tissues and chick embryo tissues were performed. In addition, quantitative semi-automated measurements were performed in the chick embryo SD-OCT images [central corneal thickness, corneoscleral junction (limbal) thickness (μm), iris thickness, anterior chamber depth (ACD), and anterior chamber area].

The measurements of corneal thicknesses across the central cornea were determined by calculating the distance between the top and bottom corneal boundaries in central segment. Similarly, the measurements were made from the region of the thickest areas for iris thickness and corneoscleral junction (limbal) thickness. The measurement of anterior chamber area was performed by marking the area of between the cornea and iris manually. The measurements of ACD across the central cornea were determined by calculating the distance between the bottom corneal and lens boundaries in central segment.

Histology

Tissue samples of the globe were fixed in 10% neutral-buffered formalin after OCT imaging for histopathologic examination. Samples were dehydrated, histologically processed, and embedded in paraffin; 5-μm thickness sections of AS were taken and stained with hematoxylin and eosin (H and E). In addition, corneal sections were stained with periodic acid–Schiff staining. Selected samples were evaluated under a light microscope (Eclipse E-600; Nikon, Tokyo, Japan).

Statistical analysis

Statistical analysis was performed with SPSS software version 18.0 (SPSS Inc., Chicago, IL, USA). Means and standard deviations were calculated for continuous variables.

Results

This proposed methodology paves the way for realizing a simple applicable morphological optical configuration for AS SD-OCT images of chick embryo consisting of conjunctiva, sclera, cornea, iris, ciliary body, and anterior chamber readings with achievable high resolution [Fig. 1].

Fig. 2a shows that the anterior surface of the cornea comprises a stratified squamous epithelium of five to seven cell layers. Epithelium lies above the Bowman's layer. White arrow indicates Bowman's layer. Black arrow indicates Descemet's membrane (DM), basal lamina of the corneal endothelial cells. Corneal stromal layer lies in between Bowman's layer and DM. The corneal stroma does not contain blood or lymphatic vessels. Endothelial cell layer can be seen just below the DM. These cells are in direct contact with the aqueous humor of the anterior chamber of the eye. Measurements of thickness

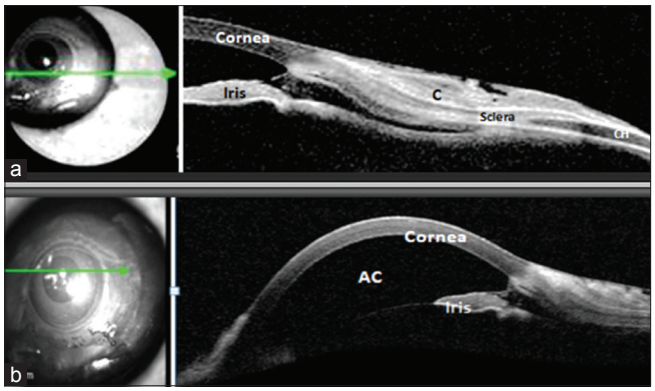

Figure 1: Representative cross-sectional spectral-domain optical coherence tomography structural images of a chick embryo anterior segment. C: conjunctiva, CH: choroid

on H and E-stained corneal cross sections are as follows: full thickness of the cornea: 220 μm, thickness of the corneal epithelium: 23 μm, thickness of the Bowman's layer: 3 μm, full thickness of stroma: 191 μm, thickness of the corneal endothelium: 4 μm, and thickness of the DM: 2 μm (H and E, ×200). When compared with histological images, SD-OCT images were able to successfully identify image distinct layers of the normal cornea (epithelium, Bowman's layer, stromal layer, and DM) [Fig. 2a-c].

The iris is the only vascularized tissue in the anterior chamber. Moreover, the iris has some specific features relevant to fluid exchange with the aqueous humor and iris volume changes. The anterior surface of the iris is not covered with endothelium; instead, a modification of the stroma with a porous surface forms the anterior surface of the human iris.[7,8] The histological layers and SD-OCT images of chick iris tissue were similar to that of human tissues. However, the stroma layer seemed to be thinner than that of human's [Fig. 3]. Interestingly, the anatomical organization and structure of the sphincter and dilatator pupil muscle and lens gross structure seemed very similar to the human iris tissue [Fig. 4].

Quantitative semi-automated measurements performed with SD-OCT device revealed the following: mean central corneal thickness: 213.4 ± 7.05 μm (197–223 μm), mean anterior chamber depth: 878.9 ± 41.74 (804–919 μm), mean anterior chamber area: 2.43 ± 0.16 mm^2 (2.17–2.73 μm), mean corneoscleral junction (limbal) thickness: 322.8 ± 20.05 μm (289–360 μm), and mean iris thickness: 230.4 ± 13.27 μm (203–245 μm) [Table 1]. Semi-automated anterior chamber area measurements were taken with marked by the line between the cornea and iris with SD-OCT [Fig. 5]. In the chick embryo eyes, the corneal thickness measured using OCT and histopathology showed similarity.

Discussion

To the best of our knowledge, this is the first preliminary study developing a novel imaging chick embryo model as an experimental animal model to assess the morphology of AS structures and morphometric measures using AS-OCT. Anatomical structures such as the cornea, anterior chamber, iridocorneal angle, and iris have been evaluated in detail using

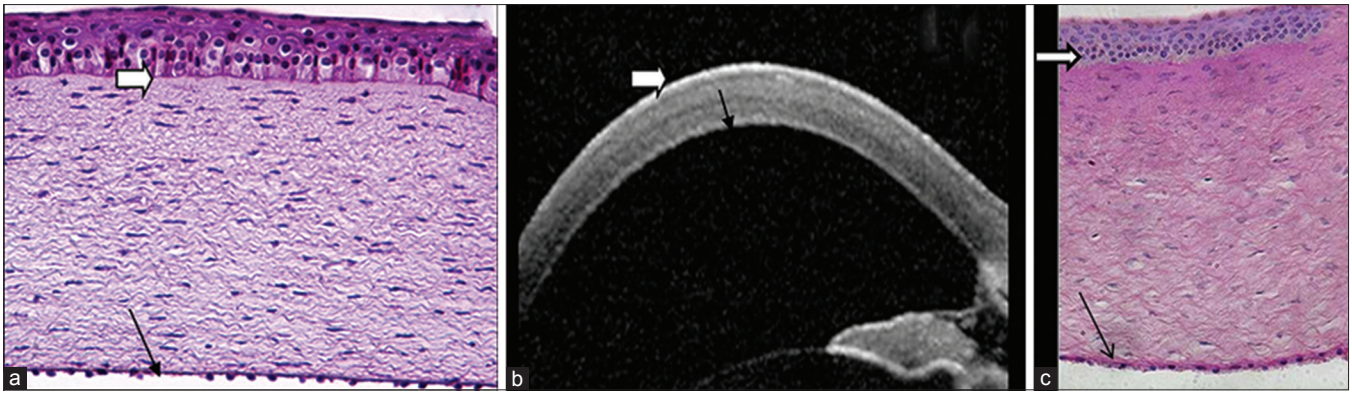

Figure 2: (a) Hematoxylin–eosin-stained corneal cross sections showing the corneal stroma and corneal surfaces covered by different types of epithelium (H and E, ×200). (b) Cross-sectional spectral-domain optical coherence tomography image, (c) Periodic acid–Schiff-stained corneal cross sections showing the corneal stroma and corneal surfaces covered by different types of epithelium (Periodic acid–Schiff, ×40). Black arrow indicates Descemet's membrane, basal lamina of the corneal endothelial cells. White arrow indicates Bowman's layer

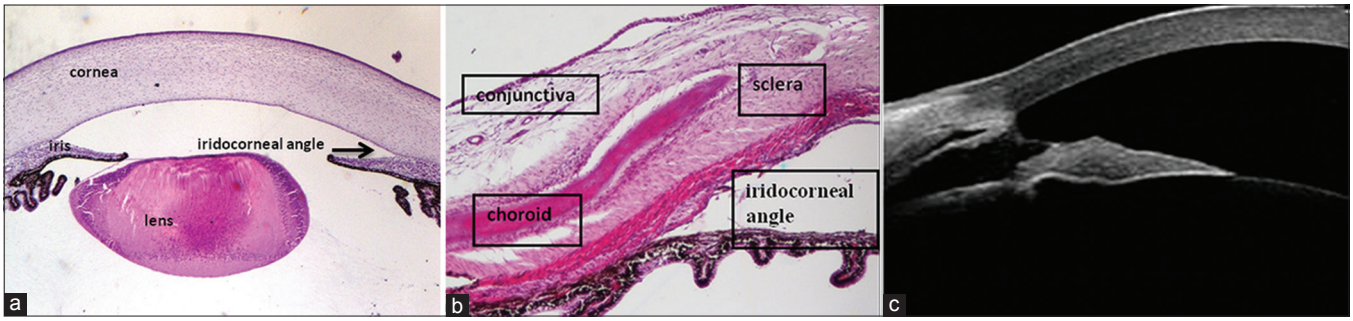

Figure 3: (a) Photomicrograph of the iridocorneal angle of the chick eye showing iridocorneal angle, cornea, iris, and lens (×4). (b) Photomicrograph of the iridocorneal angle of the chick eye showing iridocorneal angle, sclera, choroid, iris, and conjunctiva (×100). Iris has two layers; anterior pigmented fibrovascular stroma and posterior pigmented epithelial cells. (c) Cross-sectional spectral-domain optical coherence tomography images showing iridocorneal angle

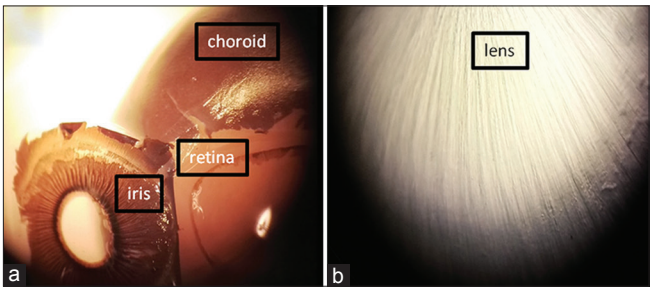

Figure 4: (a) Photomicrograph of the iris, choroid, and retina of the chick embryo eye (×10). (b) Photomicrograph of the lens tissue of the chick embryo eye (×40)

SD-OCT. These imaging findings were supported by histologic assessments conducted on the same animal model. The findings of this study showed that chick embryo AS OCT images and histopathological structure correlated strongly with human AS tissues in this model.

Rabbit, mice, rat, monkey, and pig are the most widely used experimental animals for corneal investigation. However, there are some anatomical differences between these animals and humans in AS structure.[9,10] For example, the rabbit eye used in many experimental studies is anatomically different from the human eye because of the absence of the Bowman's layer.[11-13] The sizes of the mice and rat cornea that consist of five layers are quite small when compared with human eye.[14] Although rhesus monkeys are regarded as the closest model to the human eye in terms of morphology, physiology, and pharmacological response, this model is expensive and difficult to apply. For these reasons, novel animal AS models are needed.[12]

The main advantages of using chick embryo model are being easy to handle, easily repeatable and significantly inexpensive affordable when compared to other animal models. Furthermore, the entire embryological period is completed in as little as 21 days. From the first embryological period, eye tissue can be easily disected the as the largest and easily distinguishable organ.

Several studies have shown that the anatomy and histology of the chick AS tissues are similar in size and appearance to human tissues.[9,10,15,16] Fowler WC *et al*. showed that despite the difference in collagen content, chicken corneas have the closest histologic features to humans. In addition, they found that component layer distribution (as the ratio to total thickness) of the chicken cornea was closely parallel to the human cornea. They suggested that chicken corneal wound-healing model was more compatible with human corneal physiology than current models.[9] However, in their studies, adult chickens were used.

Animal studies on the iris and iridocorneal angle have assisted in understanding the etiology of glaucoma and the development of therapies.[17-19] The changes in iris position and

Table 1: Anterior segment optical coherence tomography measurement parameters of the chick eye

Right eyes of animals	CCT (μm)	ACD (μm)	Anterior chamber area (mm²)	Corneoscleral junction (limbal) thickness (μm)	Iris thickness (μm)
Chick 1	220	823	2.44	340	239
Chick 2	221	884	2.58	360	210
Chick 3	212	915	2.62	307	240
Chick 4	213	895	2.73	326	243
Chick 5	197	913	2.40	309	237
Chick 6	210	908	2.35	328	229
Chick 7	209	804	2.17	289	203
Chick 8	223	825	2.40	342	227
Chick 9	215	903	2.38	323	245
Chick 10	214	919	2.29	304	231
Mean values±SD	213.4±7.05	878.9±41.74	2.43±0.16	322.8±20.05	230.4±13.27

CCT: Central corneal thickness, ACD: Anterior chamber depth, SD: Standard deviation

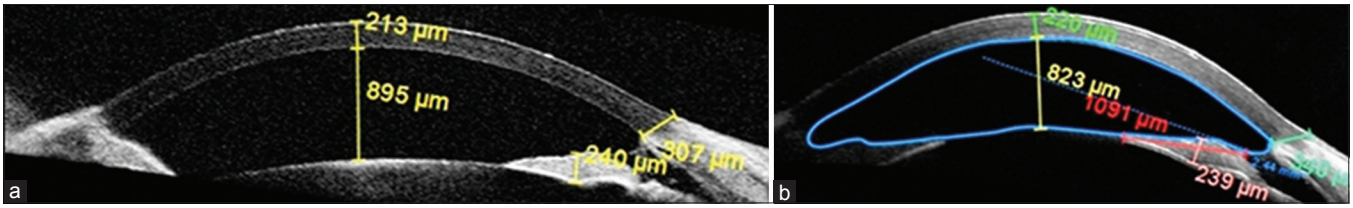

Figure 5: Cross-sectional anterior segment spectral-domain optical coherence tomography images. (a) Measurements of the thickness of the chick embryo cornea: 213 μm; anterior chamber depth: 895 μm; corneoscleral junction (limbal) thickness: 307 μm; iris thickness: 240 μm. (b) Anterior chamber area marked by blue line

volume are especially important in terms of understanding the pathogenesis of angle-closure glaucoma.[20] In addition, blood-aqueous barrier is one of the preliminary parameters for glaucoma investigations. Previous two studies reported that the chicken eye has a relatively stable blood-aqueous barrier. The stability of blood-aqueous barrier relative to experimental animals has been reported as follows: chickens ≥ ducks > rhesus monkeys ≥ owl monkeys > cats > guinea pigs ≥ rabbits.[9,12]

Histological and anatomical structure of the iridocorneal angle and iris of chick embryo is strongly similar to that in human. As iris thickness is easily measurable and the iridocorneal angle can be easily displayed in detail with SD-OCT, AS-OCT analysis in chick embryo may offer assistance in evaluating and researching the mechanisms of glaucoma, especially congenital and angle closure types.

The development of the visual system is a complex process that includes combinatorial action of many factors and cellular interactions to generate highly organized and specialized ocular structures.[21,22] According to the reported developmental staging series in the development of chick embryo, chick eye development starts at embryonic stage 9 (29–33 h after fertilization) with the formation of optic vessels.[23] The lens-placode is present at stage 14 (50–53 h) and the optic cup is shaped at stage 15 (50–55 h).[23] The main AS structures in the chick are developed before hatching.[24] In previous studies, chick embryos were sacrificed at different time points for histological and further examinations, and there is not a standard protocol for ocular assessments of the developing chick embryos.[25] Since the embryological chick has a 21-day life cycle, we analyzed the chick embryos on the 20th day of embryonic development, at complete developmental period up before hatching. However, only examination of the embryological end-stage (20th day) may be accepted as a limitation of our model. Serial assesments of different stages of embryological development might be more informative to clarify the exact developmental stages of the AS structures.

However, this study may be accepted as a pilot study showing AS OCT image similarities between chick and human eye tissues, and a detailed AS SD-OCT study covering all embryological periods might be more informative. In addition, we also recommend investigating the differences in the biochemical and physiological characteristics of the cornea and AS tissues between the chick embryo cornea model and humans in future studies.

Conclusion

In terms of ethics of animal experimentation and reduced stress to animals, our work is more acceptable and easy to apply compared with other models. This embryo model is also useful for studying the development of AS structures. This model can help understand the teratogen-induced malformations and AS dysgenesis during gestation. In conclusion, this chick embryo model mimics human tissues and it can be considered as a platform for the study of mechanisms and therapeutic agents of AS tissues. In addition, this study demonstrates the feasibility of OCT in the quantitative assessment of AS structures in chick embryo model.

Acknowledgment

All experiments were conducted in accordance with the animal research protocol of University Ethics Animal Care Committee (AKUHADYEK-235-17).

Financial support and sponsorship

Nil.

Conflicts of interest

There are no conflicts of interest.

References

1. Barabino S, Shen L, Chen L, Rashid S, Rolando M, Dana MR, *et al.* The controlled-environment chamber: A new mouse model of dry eye. Invest Ophthalmol Vis Sci 2005;46:2766-71.
2. Li N, Deng X, Gao Y, Zhang S, He M, Zhao D, *et al.* Establishment of the mild, moderate and severe dry eye models using three methods in rabbits. BMC Ophthalmol 2013;13:50.
3. Dannelly KH, Liu Y, Ghosh SK. *Pseudomonas aeruginosa* corneal infection affects cholinergic enzymes in rat lacrimal gland. Arch Microbiol 2001;177:47-53.
4. Ohadi C, Litwin KL, Moreira H, Kwitko S, Gauderman WJ, Gritz DC, *et al.* Anti-inflammatory therapy and outcome in a guinea pig model of *Pseudomonas* keratitis. Cornea 1992;11:398-403.
5. Wilkie DA, Whittaker C. Surgery of the cornea. Vet Clin North Am Small Anim Pract 1997;27:1067-107.
6. Qin Y, Tan X, Zhang Y, Jie Y, Labbe A, Pan Z, *et al.* A new nonhuman primate model of severe dry eye. Cornea 2014;33:510-7.
7. Heald K, Langham ME. Permeability of the cornea and the blood-aqueous barrier to oxygen. Br J Ophthalmol 1956;40:705-20.
8. Hogan MJ, Alvarado JA, Weddell JE. Histology of the Human Eye: An Atlas and Textbook. Philadelphia: W.B. Saunders Company; 1971.
9. Fowler WC, Chang DH, Roberts BC, Zarovnaya EL, Proia AD. A new paradigm for corneal wound healing research: The white leghorn chicken (*Gallus gallus* domesticus). Curr Eye Res 2004;28:241-50.
10. Ibares-Frías L, Gallego P, Cantalapiedra-Rodriguez R, Valsero MC, Mar S. Validation of an experimental animal model for corneal additive surgery. J Clin Exp Ophthalmol 2014;5:360.
11. Møller-Pedersen T, Cavanagh HD, Petroll WM, Jester JV. Corneal haze development after PRK is regulated by volume of stromal tissue removal. Cornea 1998;17:627-39.
12. Bito LZ. Species differences in the responses of the eye to irritation and trauma: A hypothesis of divergence in ocular defense mechanisms, and the choice of experimental animals for eye research. Exp Eye Res 1984;39:807-29.
13. Khodadoust AA, Silverstein AM, Kenyon DR, Dowling JE. Adhesion of regenerating corneal epithelium. The role of basement membrane. Am J Ophthalmol 1968;65:339-48.
14. Mohammad Nejad T, Iannaccone S, Rutherford W, Iannaccone PM, Foster CD. Mechanics and spiral formation in the rat cornea. Biomech Model Mechanobiol 2015;14:107-22.
15. Ritchey ER, Code K, Zelinka CP, Scott MA, Fischer AJ. The chicken cornea as a model of wound healing and neuronal re-innervation. Mol Vis 2011;17:2440-54.
16. Tappeiner C, Goldblum D, Katsoulis K, Sarra GM, Frueh BE. *In vivo* measurement of central corneal thickness in normal chicks (*Gallus gallus* domesticus) with the optical low-coherence reflectometer. Vet Ophthalmol 2011;14:257-61.
17. Vecino E. Animal models in the study of the glaucoma: Past, present and future. Arch Soc Esp Oftalmol 2008;83:517-9.
18. Cone FE, Steinhart MR, Oglesby EN, Kalesnykas G, Pease ME, Quigley HA, *et al.* The effects of anesthesia, mouse strain and age on intraocular pressure and an improved murine model of experimental glaucoma. Exp Eye Res 2012;99:27-35.
19. Urcola JH, Hernández M, Vecino E. Three experimental glaucoma models in rats: Comparison of the effects of intraocular pressure elevation on retinal ganglion cell size and death. Exp Eye Res 2006;83:429-37.
20. Aptel F, Chiquet C, Beccat S, Denis P. Biometric evaluation of anterior chamber changes after physiologic pupil dilation using pentacam and anterior segment optical coherence tomography. Invest Ophthalmol Vis Sci 2012;53:4005-10.
21. Graw J. Eye development. Curr Top Dev Biol 2010;90:343-86.
22. Mey J, Thanos S. Development of the visual system of the chick. I. Cell differentiation and histogenesis. Brain Res Brain Res Rev 2000;32:343-79.
23. Hamburger V, Hamılton HL. A series of normal stages in the development of the chick embryo. J Morphol 1951;88:49-92.
24. Trejo-Reveles V, McTeir L, Summers K, Rainger J. An analysis of anterior segment development in the chicken eye. Mech Dev 2018;150:42-9.
25. Lindner T, Klose R, Streckenbach F, Stahnke T, Hadlich S, Kühn JP, *et al.* Morphologic and biometric evaluation of chick embryo eyes in ovo using 7 tesla MRI. Sci Rep 2017;7:2647.